Supporting Information

Exploration of hydrated lithium manganese oxide with nanoribbon structure as cathodes in aqueous lithium ion and magnesium ion batteries

Xue Bai[a], Dianxue Cao[b], Zhuwu Jiang[a] *, Hongyu Zhang[a]*

a. College of Ecological Environment and Urban Construction, Fujian University of Technology,

Xuefu South Road, No.33, University New District, Fuzhou 350108, Fujian, P.R. China

b. Key Laboratory of Superlight Materials and Surface Technology of Ministry of Education,

College of Materials Science and Chemical Engineering, Harbin Engineering University, Nantong

street, No.145, Nangang District, Harbin, 150001, Heilongjiang, P.R. China

Supporting Information consists of one table and six figures over eight pages, which are Table S1 about the EIS values, Fig. S1 about XRD patterns corresponding to TG, Fig. S2 about CV curves, Fig. S3 about the XPS pattern for reduced electrode, Fig. S4 about XRD patterns of electrodes after different cycles, Fig. S5 about the cycle performance of full battery in lithium salt electrolyte and Fig. S6 about XRD patterns of LMO electrodes after 100 cycles in both electrolytes.

_____

*Corresponding authors.
E-mail addresses: jiangzhuwu@126.com;zhybattery@fjut.edu.cn*
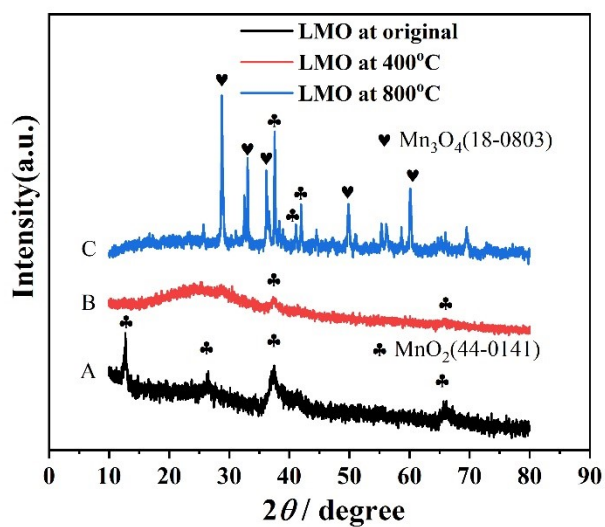
Fig. S1 XRD patterns of LMO at original, 400 ℃ and 800 ℃ corresponding to TG points A, B

and C.

The phase of LMO material is crystallized in tetragonal phase (JCPDS No. 44-0141).

Combining with the TG graph, the structure of LMO collapses when it heats at 400 ℃

and the XRD peak at $2\theta = 12.7°$ of main structure loses. When the temperature at 800

℃, it can be found that the most parts of LMO phase transforms to Mn_3O_4 with the

JCPDS No. 18-0803.
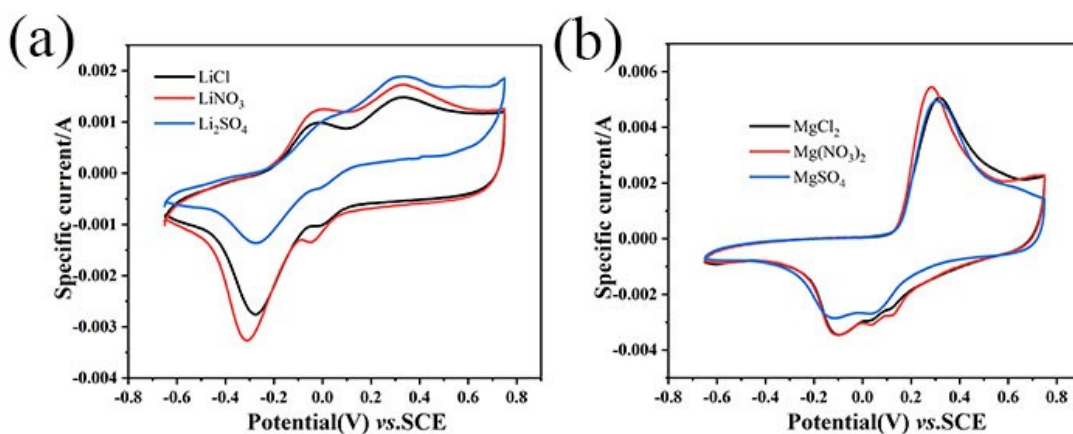
Fig. S2 The CV curves of electrodes at 1 mV s^{-1} in lithium salt (a) and magnesium salt (b)

electrolytes.

Fig. S2 exhibit the cyclic voltammograms (CVs) of LMO electrodes in lithium salt (a) and magnesium salt (b) electrolytes at the scan rate of 1 mV s^{-1} in the potential window from −0.65 to 0.75 V, which uses to investigate the behaviors of Li$^+$ and Mg^{2+} insertion/deinsertion. It can be found that the LMO electrode shows the best electrochemical performance in LiNO$_3$ and Mg(NO$_3$)$_2$ electrolytes, respectively. Meanwhile, the position of redox peaks corresponds to the charged and discharged platforms. The reduction/oxidation couples peaks are resulted from the donor and acceptor of electrons accompanying the Li$^+$/Mg^{2+} ions insertion/deinsertion processes into the lattice of LMO electrodes.

**Table S1** Evaluated impedance parameters, σ and $D_{Mg}{}^{2+}$ values in the different electrolytes

solution	$R_s(\Omega)$	CPE-T	CPE-P	$R_{ct}(\Omega)$	σ	$D_{Mg}{}^{2+}(cm^2 s^{-1})$
0.5 mol·dm^{-3} MgCl$_2$	2.327	0.000124	0.656	5.263	5.055	3.231E-16
0.5mol·dm^{-3}Mg(NO$_3$)$_2$	2.078	0.000572	0.7137	4.082	4.860	3.593E-16
0.5 mol·dm^{-3} MgSO$_4$	4.542	0.000721	0.6801	11.86	5.933	2.411E-16

Table S1 list the EIS parameters of this electrodes in three magnesium salt electrolyte, which is fitted by the ZView software. The obtained magnesium ion diffusion coefficient ($D_{Mg}{}^{2+}$) of this electrode in 0.5mol·dm^{-3}Mg(NO$_3$)$_2$ is larger than that of in other two electrolytes, demonstrating that this cathode shows more excellent electrochemical properties.
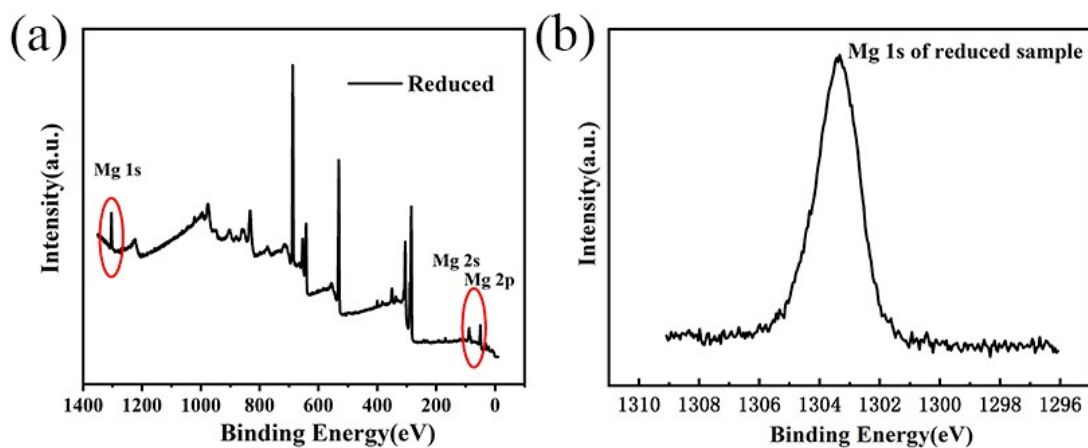
Fig. S3 The XPS pattern of reduced electrode (a), and Mg 1s core level spectra (b).

It can be found that after the discharged process, the magnesium ion insert into the lattice of host material in Fig. S3, which accompanied by the changed valence of manganese based on the literatures about the manganese dioxide material as electrode.
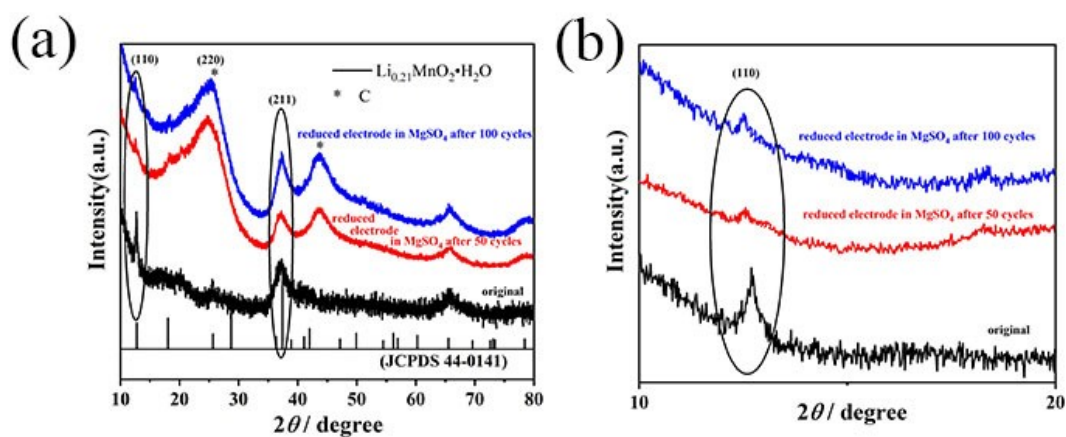
Fig. S4 XRD patterns of the original, reduced electrode at 100 mA g^{-1} -0.65 V after 50 cycles and reduced electrode after 100 cycles (a) and its enlarged view at 10°~20° (b).

Fig. S4a shows the XRD patterns of original LMO powder (black lines), reduced electrode coating on the carbon fiber cloths after 50 cycles (red lines) and reduced electrode coating on the carbon fiber cloths after100 cycles (blue lines). It can be found that the (110), (211) peaks of three samples are still existed, indicating that the structure of LMO has not changed after 50 or 100 cycles. Meanwhile, the XRD peak of reduced electrode shift to low angle direction (Fig. S4b), which manifests that lots of magnesium ions insert into the lattice of LMO electrode after discharged process and the LMO gives the intercalation mechanism in Mg storage.
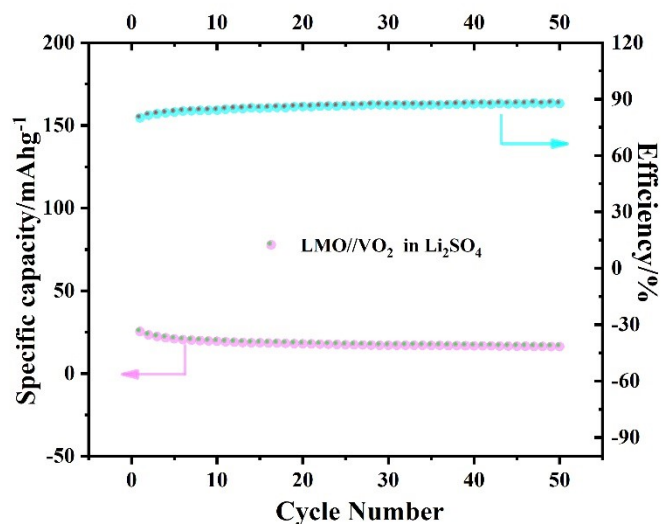
Fig. S5 The cycle performance of aqueous lithium ion battery based on LMO as cathode and VO_2

as anode.

Fig. S5 gives the cycle performance of LMO as cathode and VO_2 as anode in 0.25 mol

dm^{-3} Li_2SO_4 electrolyte from the voltage window of 0V to 1.6 V. It can be found that

The discharged capacity of this device in Li_2SO_4 electrolyte at 100 mA g^{-1} after 50

cycles decreases from 25.4 to 16.3 mAh g^{-1}, corresponding to a capacity retention of

64.2%, which also exhibits an unsatisfactory result than that of in magnesium ion

electrolyte system.
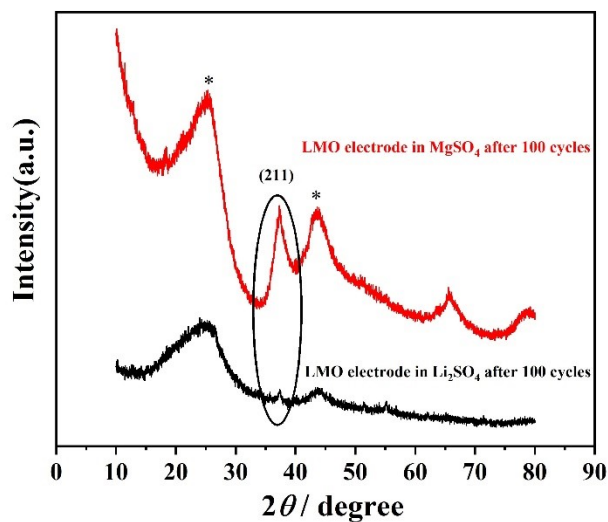
Fig. S6 XRD patterns of reduced electrodes in Li$_2$SO$_4$ and MgSO$_4$ electrolytes after 100 cycles.

Comparing with the XRD patterns of LMO electrodes in Li$_2$SO$_4$ and MgSO$_4$ electrolytes, it still can be found the main peak of (211) plane with high intensity for LMO electrode in MgSO$_4$ electrolytes, proving that the structure is beneficial for LMO electrode to exhibit more excellent electrochemical performance in magnesium salt electrode than that in lithium salt electrolyte.